Electronic Materials Letters, Vol. 3, No. 2 (2007), pp. 69-74

Mechanism of Enhanced Crystallization of Amorphous Si Thin Films by Microwave Annealing

Jin Hyung Ahn[1] and Byung Tae Ahn[2,*]

[2]Department of Materials Science and Engineering, Korea Advanced Institute of Science and Technology, 373-1, Guseong-dong, Yuseong-gu, Daejeon 305-701, Korea.
[1]LG Electronics Institute of Technology, Seoul 137-724, Korea

The crystallization of amorphous Si thin films was enhanced by applying microwaves to the films. The mechanism of the enhanced crystallization was investigated by analyzing the nucleation and growth behavior of polycrystalline Si films from a $NiCl_2$-coated a-Si film that was deposited using a Si_2H_6 gas. It was found that both the nucleation rate and growth rate of crystal Si were enhanced by the microwave annealing, compared to conventional furnace annealing. The activation energy of the nucleation rate was lowered from 2.94 to 2.50 eV and the activation energy of lateral growth velocity was lowered from 2.12 to 1.55 eV. From the results, it is considered that the enhanced crystallization is not due to the heat supplied by microwave annealing but due to the enhanced mobility by an ac field that is imposed on the Si thin film.

Key words: polycrystalline Si film, metal induced crystallization, microwave annealing, solid phase crystallization

1. INTRODUCTION

Polycrystalline Si (poly-Si) thin films for application to display devices are generally fabricated by crystallizing amorphous Si (a-Si) thin film precursors. Two competing types of crystallization technologies are currently available: laser crystallization and non-laser crystallization. Among non-laser crystallization methods, solid phase crystallization (SPC), in which a-Si films are annealed without melting, has been widely studied and is gradually being commercialized. In the SPC process, lowering the crystallization temperature is the most challenging task, as the glass substrate can then be properly employed. A common approach is the application of metal film onto the surface of amorphous Si thin films followed by an annealing treatment in a furnace, resulting in a lower crystallization temperature (metal-induced crystallization, MIC)[1]. Ni is widely used in the MIC process as it readily forms $NiSi_2$, which is nearly isomorphic and has only a slight lattice mismatch with crystalline Si. In this case, Si is dissolved into $NiSi_2$ and is precipitated as crystal Si in a process known as silicide-mediated crystallization (SMC)[2]. When Ni metal is applied onto a selected region of a-Si film, the crystallization laterally propagates to the a-Si region where no Ni is supplied in a process known as metal-induced lateral crystallization (MILC)[3]. The difference between SMC and MILC is that Ni metal is located directed on the a-Si film in SMC, while Ni metal is not positioned on the a-Si film in MILC. A high-performance thin-film transistor through MILC processing of the channel area with an SMC source/drain area onto a 0.5-nm thick Ni film was reported[3]. To enhance SMC and MILC, several methods have been reported, including rapid thermal annealing[4], annealing with a DC bias[5,6], and annealing within a RF furnace[7]. In addition, Lee *et al*. reported microwave annealing as an alternative method of enhancing crystallization[8,9].

The authors of the present study have utilized a metal solution as a metal source, instead of metal film, in order to minimize metal contamination in Si films[1,10]. However, the crystallization time is much longer in this case due to the low metal concentration in contact with the a-Si film. Therefore, the application of microwave annealing may be as effective as the a-Si film without metal[8]. $NiCl_2$-coated a-Si films were crystallized with microwave annealing, and enhanced crystallization by the synergistic effect of SMC and microwaves was observed. With microwave annealing, a complete understanding of the crystallization mechanism is not yet known. This paper reports a kinetic analysis of the crystallization behavior and details the influence of microwave heating on the crystallization of a-Si films.

2. EXPERIMENTS

100-nm thick a-Si films were deposited on oxidized Si wafers by LPCVD using Si_2H_6 at 530°C. The a-Si films were

*Corresponding author: btahn@kaist.ac.kr

cleaned in a boiling H_2SO_4+H_2O_2 solution and dipped in a diluted HF solution to remove native and chemical oxides on the surface. Ni was supplied onto the a-Si films in the form of $NiCl_2$ from a Ni solution fabricated by dissolving $NiCl_2$ in a mixture of 1 N HCl + propylene glycol. $NiCl_2$ is less reactive to Si than Ni metal, thus the crystallization temperature of $NiCl_2$-coated a-Si film is slightly higher than that of a Ni-coated a-Si film [10]. For MILC, a SiO_2 mask layer was deposited and patterned prior to $NiCl_2$ coating.

Specimens prepared as above were annealed in a microwave furnace system. This system consists of a microwave generator and an applicator in which specimens are charged. Microwaves at a frequency of 2.45GHz were supplied from a microwave generator to an applicator in a nitrogen atmosphere through a wave guide. Specimens were put on a tray consisting of a Si wafer and the backside temperature of the specimen was monitored with a thermocouple device. The specimens were also annealed in a conventional tube furnace for comparison.

The crystalline fraction in the Si films was measured via the (111) intensity of X-ray diffraction (XRD), and scanning electron microscope (SEM) images were observed after etching off non-crystallized a-Si regions with a Si-defect etchant (1.75M : 1 : 100 CrO_3 + 49%HF + H_2O). The extent of the lateral crystallization was measured by the length of the crystallized area beneath the SiO_2 mask, which was observed through an optical microscope.

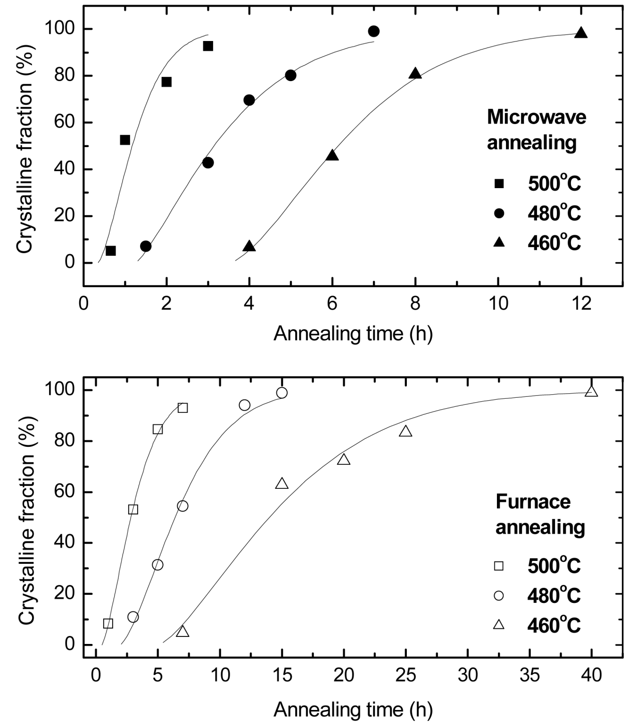

Fig. 1. Crystallization behavior of $NiCl_2$ coated a-Si films with furnace annealing and microwave annealing at various temperatures.

3. RESULTS AND DISCUSSION

Figure 1 shows the SMC behavior of $NiCl_2$-coated a-Si films with microwave annealing and furnace annealing at 460, 480 and 500°C. It is interesting to note that, with the microwave annealing, the crystallization was enhanced at all temperatures. At 480°C, approximately 3% of crystallization progressed after 2 h of annealing. Crystallization was completed after 15 h by furnace annealing. On the other hand, nearly 7% of the crystallization had progressed after 1.5 h, and the crystallization process was completed after 7 h by microwave annealing. The crystallization time was shortened by one half and the effect was greater as the temperature decreased.

The solid lines in Fig. 1 are the fitting results with the Avrami-John-Mehl (AJM) equation. The crystallization behaviour can be systemically compared using kinetic parameters extracted from the model that can be expressed by the following AJM equation [11],

$$\mathbf{X_T} = \mathbf{1} = \exp\left[-\left(\frac{\mathbf{t}-\mathbf{t_0}}{\mathbf{t_c}}\right)^{\mathbf{n}}\right]$$

Here, X_T is the crystalline fraction, t is the annealing time, t_0 is the incubation time, t_c is the crystallization time, and n is the exponent that depends on the crystallization mechanism. The t_o value denotes the time at which nucleation starts and X_T equals 0.63 at the time $t = t_o + t_c$. The inverse of t_o is reported to be proportional to the nucleation velocity [11], and the crystallization time t_c is determined by crystallization mechanism as well as by the nucleation and growth rate [12]. Lee *et al*. derived the Avrami-John-Mehl equation in the case that nucleation begins at limited active sites [13].

During the SMC process, crystallization occurs at defined sites of $NiSi_2$ precipitates. At these sites, the crystalline Si grains grow linearly, resulting in the needle-like grains. The growth of c-Si grains is limited by the diffusion of Ni atoms thorough $NiSi_2$ precipitates [2]. Under this condition, the exponent n has a value between 1 and 2 corresponding to cases of very slow nucleation and very fast nucleation, respectively. Lam *et al*. experimentally reported the exponent of 1.5 for SMC [4]. In the present study, n is in good agreement with the value between 1.4 ± 0.1. As the crystallization process of the a-Si film deposited by Si_2H_6 gas is much slower than that of the a-Si film deposited by SiH_4 gas, this is expected to be close to 1. However, microwave annealing enhanced the crystallization, resulting in an increase in the exponent to 1.4.

t_o can then be extracted from the AJM equation for the furnace annealing and microwave annealing. The t_o values for the three furnace annealing conditions are 11.6, 5.72 and 3.05 h. These values for the microwave annealing at 460, 480 and 500°C are 3.51, 1.25 and 0.35 h, respectively. The

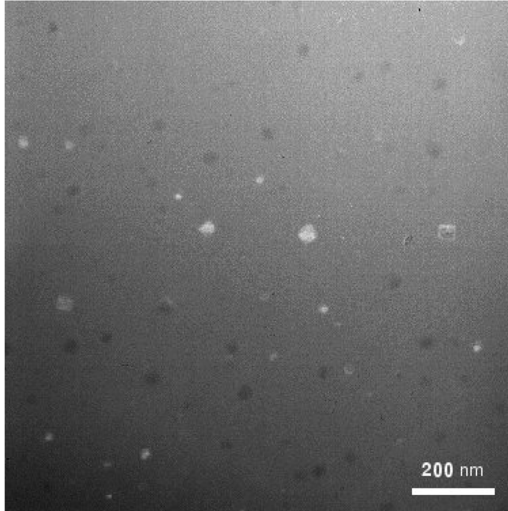

Fig. 2. $NiSi_2$ precipitates in Si films annealed at 450°C for 5h under furnace annealing.

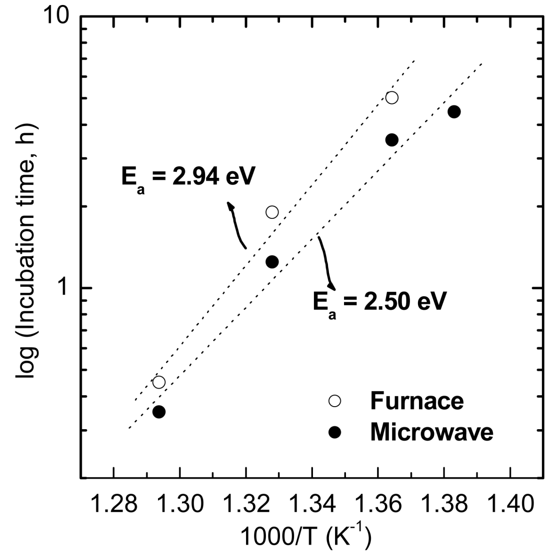

Fig. 3. Arrhenius plot of the incubation time of crystallization with microwave and furnace annealing.

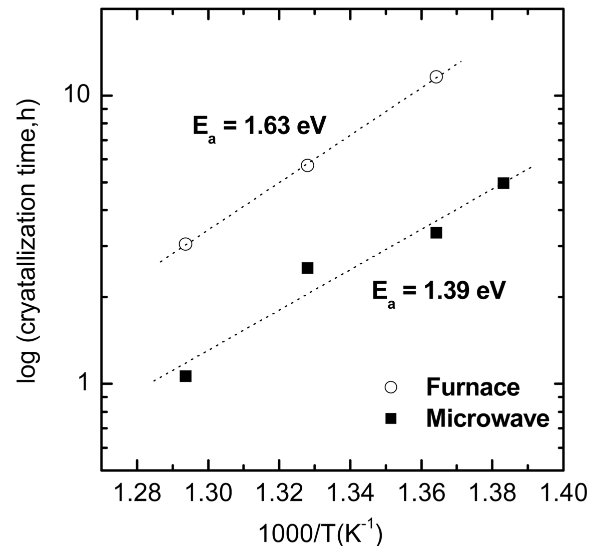

Fig. 4. Arrhenius plot of the crystallization time of crystallization with microwave and furnace annealing.

crystallization time, t_c, can also be extracted from the equation for the furnace annealing and microwave annealing. The t_c values for the furnace annealing at 460, 480 and 500°C are 5.02, 1.90, and 0.45 h, respectively. These values for the microwave annealing at 460, 480 and 500°C are 3.34, 2.52 and 1.06 h, respectively.

Reviewing the Ni-SMC mechanism, a crystalline Si nucleates on (111) surfaces of $NiSi_2$ precipitate due to the very good match at the (111) face. From the top view, the shape of NiS_2 changes from a circle to a long rectangle to maximize the (111) interface area. The Si grain grows along the [111] direction with the $NiSi_2$ growth front. This results in needle-like grains. The growth of c-Si grains is limited by the diffusion of Ni atoms thorough $NiSi_2$ precipitates [14].

Figure 2 shows (a) the $NiSi_2$ precipitates in Si films annealed at 450°C for 5 h by furnace annealing, and (b) the polycrystalline Si grains after the completion of the SMC process at 480°C. This annealing condition is well below the incubation time because the estimated incubation time at 450°C with furnace annealing is approximately 10 h. In Fig. 2, 4.5×10^9 /cm^2 of the $NiSi_2$ particles are precipitated while no c-Si is formed. Cammarata *et al*. also reported that $NiSi_2$ precipitation occurs immediately at the initial stage of annealing, even at temperatures lower than those at which the growth of c-Si begins [15].

Nucleation consists of two steps: the precipitation of $NiSi_2$ and the heterogeneous nucleation of crystalline Si on the surface of $NiSi_2$ precipitate [15]. However, the precipitation of $NiSi_2$ (preferential nucleation sites) are already given with a concentration of 4.5×10^9/cm^2. Thus, during the nucleation of Ni SMC, it can be considered that the heterogeneous nucleation of c-Si on pre-existing $NiSi_2$ precipitates is the rate-limiting step.

Figure 3 shows an Arrhenius plot of the incubation time of SMC [log t_o vs. 1000/T] with furnace annealing and microwave annealing. The activation energies of the incubation time by furnace annealing and microwave annealing are 2.94 and 2.50 eV, respectively. The activation energy is lowered by 0.44 eV by microwave annealing. The reduction of the activation energy of the incubation time indicates that the activation energy of the nucleation rate is reduced with microwave annealing. This result shows that microwave annealing enhances the heterogeneous nucleation of c-Si on $NiSi_2$ precipitates.

Figure 4 shows an Arrhenius plot of the crystallization

time of SMC with furnace annealing and microwave annealing. The activation energy of the crystallization time with furnace annealing and microwave annealing are 1.6 and 1.4 eV, respectively. The activation energy of the crystallization is also reduced by microwave annealing. Lam *et al*. reported 1.84 eV for the crystallization time of Ni SMC using a Ni metal layer in a temperature range of 560 to 600°C by furnace annealing [4]. The difference is due to the difference in the source gas and the deposition temperature. Given that the activation energy reflects both nucleation and grain growth and that most grains impinge upon each other at this time, it is difficult to isolate the growth rate from the crystallization fraction.

The effect of annealing on the growth of the grains can be estimated by the MILC behaviour, during which existing grains grow in one direction overall. Figure 5 shows (a) a SEM image of a growth front of a MILC poly-Si film crystallized at 500°C for 10 h, and (b) a TEM image of the tip of a needle-like grain of a MILC poly-Si film. As seen in Fig. 5b, it is well known that a $NiSi_2$ precipitate exists between the crystalline Si and a-Si, and that the growth front of the needle-like grains always consists of the $NISi_2$ precipitate. However, the growth direction of the needle-like grains of MILC poly-Si differs from that of the macroscopic MILC growth direction, as seen in Fig. 7a. The individual grains are merged together and the c-Si grows toward a-Si region [16]. Although the growth rate of individual grain differs from that of the c-Si film, the overall direction of the grains is identical to that of c-Si. By measuring the length of the c-Si grown by the MILC process, the average growth rate of individual grains can be calculated.

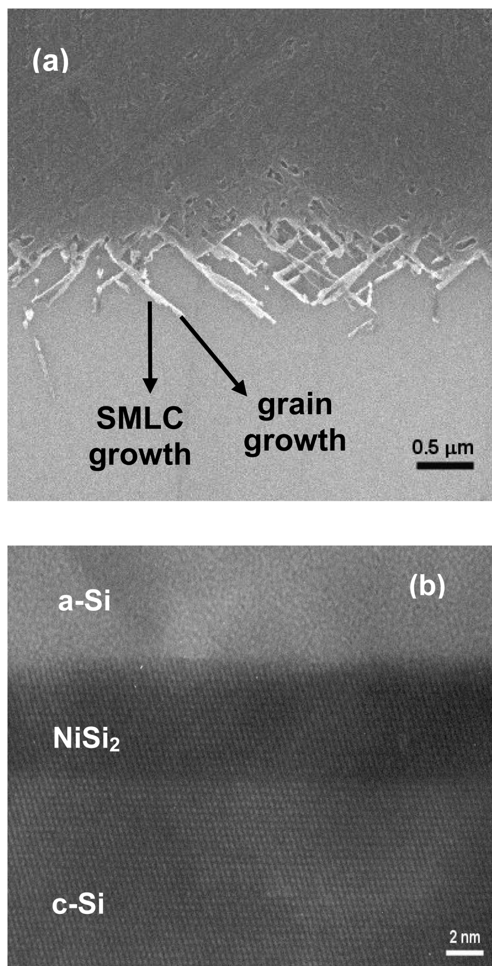

Fig. 5. (a) SEM image of a growth front of a SMLC poly-Si film, and (b) TEM image of the tip of a needle-like grain of a SMLC poly-Si film annealed at 500°C for 10h.

Figure 6 shows the lateral-crystallization length of the c-Si area by the MILC process with microwave annealing and furnace annealing at various temperatures. At 530°C for 7 h, the length of the laterally crystallized area with microwave annealing is 24.0 μm, while that with furnace annealing is 7.7 μm. The length of the laterally crystallized region with microwave annealing is generally more than three times larger, although this depends on the annealing time and temperature. The growth length of the c-Si area by the MILC process can be fitted with a line for each temperature, and the lateral crystallization velocity can be extracted from the slope of the line. The MILC velocities by microwave annealing at 500, 515, 530 and 550°C are 1.95, 3.01, 4.50 and 8.07 μm/h, respectively, while those by furnace annealing are 0.68, 1.12, 1.43 and 4.37 μm/h, respectively.

Figure 7 shows an Arrhenius plot of the velocity of lateral crystallization as function of the crystallization temperature. The slope of the plot represents the activation energy of the velocity of lateral crystallization or the average growth rate of the grains. The activation energies by furnace annealing and microwave annealing are 2.12 and 1.55 eV, respectively. Lam reported 1.86 eV of activation energy for the lateral

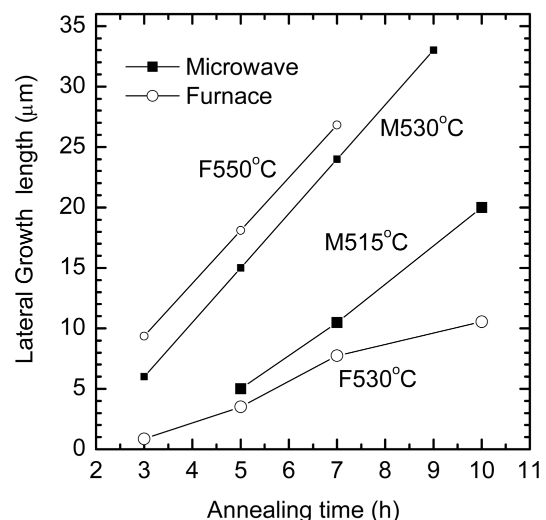

Fig. 6. Lateral-crystallization length with microwave and furnace annealing at various annealing temperatures.

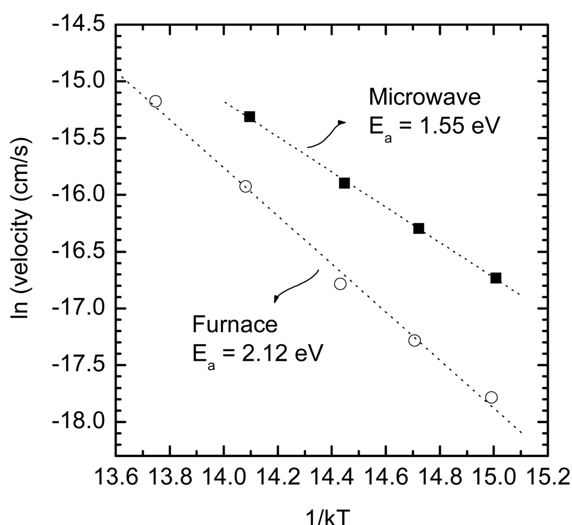

Fig. 7. Arrhenius plot of the velocity of lateral crystallization at various crystallization temperatures.

crystallization velocity by furnace annealing[4]. As the a-Si film was deposited by Si_2H_6, the activation energy is expected to be larger than Lam's result. However, the activation energy is lowered by microwave annealing. In this case, the activation energy is lowered by 0.57 eV as a result of microwave annealing. The reduction of the activation energy of the MILC velocity implies that the activation energy of the grain growth rate is reduced. Thus, the result in this study shows that microwave annealing enhances not only the nucleation rate but also the grain growth rate, compared to furnace annealing.

The reduced activation energies for both the nucleation rate and grain growth rate suggest that microwave annealing not only supplies heat to the Si substrate but also enhances the atomic mobilities through the $NiSi_2$ precipitates. This mobility enhancement may originate from the interaction of the microwave ac field and the mobile species, resulting in an additional supply of energy to the mobile species. In other words, electric-field agitation significantly enhances Si diffusion through $NiSi_2$ precipitates. The same phenomenon is related to the rapid evolution of hydrogen from a-Si films during microwave annealing[8]. An enhancement of the diffusion rate and reaction rate by microwave annealing can be also found in ceramic systems [17,18], and the enhanced mass transport in NaCl single crystal takes place through the increase of the ionic current[19].

4. CONCLUSIONS

The mechanism of enhanced crystallization resulting from a microwave application was investigated through a kinetic study of crystallization. Ni SMC and Ni MILC were conducted by coating $NiCl_2$ onto a-Si as deposited from Si_2H_6 gas and annealing the sample in a microwave furnace. During the SMC process, it was found that $NiSi_2$ particles were formed immediately while the nucleation of Si grains from the particles was slow. From the incubation time of Si grains with various annealing temperatures, the nucleation activation energy was calculated. The nucleation activation energy was reduced from 2.94 eV to 2.50 eV by microwave annealing compared to conventional furnace annealing. The grain growth rate was calculated from the growth velocity of Si grains during the MILC process, and the activation energy of the grain growth was found to be reduced from 2.12 eV to 1.55 eV by microwave annealing compared to conventional furnace annealing. As indicated by the fact that activation was reduced less by microwave annealing, it is concluded that the enhanced crystallization by microwave application is not due to the heat supplied via microwave annealing but is instead due to the enhanced mobility by the ac field imposed on the Si thin film.

ACKNOWLEDGMENT

This work was financially supported by the Korea Research Foundation through the Center for Nano Interface Technology at KAIST.

REFERENCES

1. D. K. Sohn, J. N. Lee, S. W. Kang, and B. T. Ahn, *Jap. J. Appl. Phys.* **35**, 1005 (1996).
2. C. Hayzelden, J. L. Batstone, and R. C. Cammarata, *Appl. Phys. Lett*. **60**, 225 (1992).
3. S. W. Lee and S. K. Joo, *IEEE Electron Device Letters* **17**, 160 (1996).
4. L. K. Lam, S. Chen, and D. G. Ast, *Appl. Phys. Lett.* **74**, 1866 (1999).
5. S. I. Jun, Y. H. Yang, J. B. Lee, and D. K. Choi, *Appl. Phys. Lett*. **75**, 2235 (1999).
6. J. Jang, J. Y. Oh, S. K. Kim, Y. J. Choi, S. Y. Yoon, and C. O. Kim, *Nature* **395**, 481 (1998).
7. K. H. Kang, S. H. Park. S. J. Lee, S. E. Nam, and H. J. Kim, *J. Inform. Display* **4**, 34 (2003).
8. J. N. Lee, Y. W. Choi, B. J. Lee, and B. T. Ahn, *J. App. Phys*. **82**, 2918 (1997).
9. J. H. Ahn, J. N. Lee, Y. C. Kim, and B. T. Ahn, *Curr. Appl. Phys*. **2**, 135 (2002).
10. J. H. Ahn and B. T. Ahn, *J. Electrochem. Soc*. **148**, H115 (2001).
11. I. W. Wu, A. Chiang, M. Fuse, L. Ovecoglu, and T. Y. Huang, *J. Appl. Phys*. **65**, 4036 (1989).
12. K. N. Tu, J. W. Mayer, and L. C. Feldman, *Electronic Thin Film Science*, p. 261, Macmillan Publishing Company (1992).
13. J. G. Lee, W. H. Jin, E. G. Lee, and I. G. Lim, *Korean. J. Mater. Res*. **6**, 309 (1996).

14. C. Hayzelden and J. L. Batstone, *J. Appl. Phys.* **73**, 8279 (1993).
15. R. C. Cammarata, C. V. Thompson, C. Hayzelden, and K. N. Tu, *J. Mater. Res*. **10**, 2133 (1990).
16. J. H. Ahn, J. H. Eom, and B. T. Ahn, *J. Electrochem. Soc*. **151**, H141 (2004).
15. M. A. Janney, H. D. Kimrey, M. A. Schmiat, and J. O. Kiggan, *J. Am. Ceram. Soc*. **74**, 1675 (1991).
16. D. A. C. Stuerga and P. Gaillard, *J. Microwave Power and Electromagnetic Energy* **31**, 87 (1996).
17. S. Freeman, J. Booske, R. Cooper, and B. Meng, *Mat. Res. Symp. Proc*. **347**, 479 (1994).
18. J. H. Booske, R. F. Cooper, and I. Dobson, *J. Mater. Sci*. **7**, 495 (1992).
19. K. I. Rybakov and V. E. Semenov, *Phys. Rev. B* **49**, 64 (1994).